Electrodeposition of PbO_2 on glassy carbon electrodes: influence of ultrasound power

José González-García*, Verónica Sáez, Jesús Iniesta, Vicente Montiel and Antonio Aldaz

Grupo de Electroquímica Aplicada, Departamento de Química Física

Universidad de Alicante, Ap. Correos 99. 03080 Alicante, Spain

ABSTRACT

The influence of the ultrasonic intensity on the electrocrystallisation of lead dioxide on glassy carbon electrodes was studied in 1 mol dm^{-3} HNO_3 + 0.1 mol dm^{-3} $Pb(NO_3)_2$. Chronoamperometry and numerical approximations of the current transients have been carried out in order to compare these results with those obtained in the absence of ultrasound. Results show different effects of the ultrasound power from those obtained with other variables like electrode potential.

Key words: ultrasound, lead dioxide, glassy carbon electrodes, sonoelectrochemistry, electrodeposition nucleation.

1. Introduction

The preparation of lead dioxide anodes is an active research field because of the diversity of applications in batteries [1], wastewater treatment by electrooxidation of

* Corresponding author. Tel. +33985903855; fax +33965903537. E-mail: jose.gonzalez@ua.es

organics [2,3], ozone generation [4], electrosynthesis [5] and electrowinning of metals [6] of this type of anodes.

PbO_2 anodes are normally prepared by electrochemical methods [7] and so, the electrocrystallization process is a crucial step determining the electrochemical behaviour of this type of anodes, both from a fundamental point of view and for industrial uses, i.e. anodes with adequate electrocatalytic properties and long life. Several mechanisms for lead dioxide electrodeposition involving adsorbed [8-11] and/or soluble intermediates [12-18] have been proposed. Recent results have pointed out the complexity of lead dioxide electrodeposition mechanism itself related to mass transport versus lattice incorporation for different experimental conditions [19, 20] and to interference caused by oxygen evolution at high anodic overpotentials [21].

The influence of ultrasound on the electrochemical behaviour of different systems is also an active field of research [22, 23]. High intensity ultrasonic irradiation generates different chemical and physical effects that can produce important modifications in electrochemical processes. Thus physical effects, such as mass transport enhancement [24] and surface cleaning [25], as well as chemical effects such as formation of radicals $OH^{\cdot}$ and $H^{\cdot}$ due to sonolysis of water [26] have been reported in the literature.

The influence of ultrasound on the electrodeposition of lead dioxide is being currently studied in our laboratory. Previous work [27-30], using a typical laboratory cleaning ultrasonic bath in which the electrochemical cell was placed, has shown important effects of ultrasound on the kinetics of the electrodeposition process of lead

dioxide. However, the use of such type of ultrasonic bath has several drawbacks such as work to a fixed nominal frequency and ultrasonic power, defective distribution of the sonic field, absorption of the sonic waves by the glass walls etc. Therefore, the results strongly depend on the design of the electrochemical cell and on its position inside the ultrasonic bath. This paper presents a preliminary study of the influence of the ultrasonic power on the electrodeposition process of lead dioxide using a sonoreactor with variable ultrasound power, better ultrasonic field distribution and absence of absorption of the ultrasound waves by the glass walls.

2. Experimental

The chronoamperometric curves were obtained using a Voltalab electrochemical system with a DEA 332 potentiostat and an IMT 102 electrochemical interface, connected to a PC for data acquisition and control. As working electrode a glassy carbon rod CV25 (3 mm diameter.) from Sofacel (Le Carbone-Lorraine) was used. The glassy carbon rod was sheathed by two cylinders of Teflon. The first one was fitted thermically. The second cylinder (to provide a wide sheath) was fitted by pressing. The counter electrode was a spiral wounded platinum wire. All potentials were measured with reference to a saturated calomel electrode (SCE) (Radiometer, Copenhagen) connected to the electrochemical cell via a Luggin capillary.

The sonoelectrochemical reactor consisted of a jacketed Sonoreactor® (20 kHz, 100 W maximum power) supplied by Undatim. This system was electrically isolated and was calibrated by the calorimetric method in a previous work [31] . A sketch of the experimental cell is shown in figure 1. In order to maintain the electrochemical system

at a constant temperature, an additional cooling glass coil system (not shown in figure 1), connected in series to the jacket, was introduced in the solution. In order to minimise ultrasonic field perturbations the coil was fitted to the inner wall of the sonoreactor. The temperature was maintained constant to 22±1ºC and monitored with a thermocouple. The ultrasound source is fitted at the bottom of the cell, so the working electrode-ultrasound horn configuration was "face on". The separation distance, d, between the Ti horn (30 mm diam.) and the surface of the glassy carbon electrode was 1 cm in all experiments.

Before each experiment, the glassy carbon electrode was polished with decreasing size alumina powder (1, 0.3 and 0.05 μm) until a mirror finish was obtained. After that, the electrode was thoroughly rinsed with ultrapure water. During the sonication time, it was not detected any damage by visual inspection and SEM micrographs with this type of glassy carbon electrode. The electrolyte was deoxygenated to eliminate oxygen and after that saturated with Ar in order to have the same amount of gas in the electrolytic during the experiments. Also, to avoid possible interference caused by oxygen introduction a current of Ar was maintained on the surface of the electrolyte during the experiments. After each experiment, the lead dioxide deposit was stripped from the surface using a 1:1 mixture of acetic acid and hydrogen peroxide followed by rising with water. The concentration of the solution employed for the chronoamperometry study was 0.1 mol dm^{-3} lead (II) nitrate (Merck a.r.) + 1 mol dm^{-3} nitric acid (Merck a.r.). The total volume was 200 mL. The solutions were prepared using ultrapure water from a Millipore Mill-Q system.

3. Results and Discussion

Figure 2 shows the chronoamperometric curves for PbO_2 deposition from Pb(II) solutions on a glassy carbon electrode recorded under silent and ultrasonic conditions and for different ultrasound intensities at a step final potential of 1.480 V *vs* SCE. In these experimental conditions, the deposition process takes place in the nucleation control zone [20]. It is clearly shown that in silent conditions no electrodeposition process takes place. The electrodeposition of lead dioxide is a very complex process and is strongly influenced by pH, temperature and potential applied. Besides, the surface state of the electrode is crucial as well. So, a carefully statement of the experimental conditions is very important. We normally use experimental conditions where the electrodeposition process is not favoured (pH very low, low Pb(II) concentration…) [20, 27-30]. In these experimental conditions, the mass transport enhancement does not cause the nucleation process. In fact, at higher electrode potentials where the electrodeposition begins to take place, an enhancement of mass transport decreases the process [20]. However under sonication, nucleation and growth of the lead dioxide deposit occurs showing a strong influence of the irradiation power on the deposit process. Well S-shaped curves are obtained with very well defined plateau currents. An increase of power ultrasound (figure 2) and electrode potential (figure 3) has a strong influence on lead dioxide electrodeposition but not in the same way. Thus when the ultrasound power increase a faster growth of the deposits takes place being the currents of the plateau independent of the ultrasound intensity. However both the rate of crystallisation and the plateau currents increase when the end potential of the step is increased.

The kinetic parameters of electrocrystallization processes can be obtained by modelling of the experimental curves using the different models proposed in the literature. Between the different models the best agreement was obtained for the simple progressive 3D nucleation and crystal growth model with the outward growth on a substrate base plane surface not covered by growing nuclei. The relation j vs t is [32]:

$$j = j_0 \exp\left[-\frac{\pi M^2 k N_0 A}{3\rho^2}(t - t_0)^3 \right] + zFk\left[1 - \exp\left[-\frac{\pi M^2 k N_0 A}{3\rho^2}(t - t_0)^3 \right] \right] \quad (1)$$

This equation contains four parameters: t_0 (s), the induction time; j_0 (mA cm^{-2}), the current density in the induction time; k (mol cm^{-2} s^{-1}), the growth rate constant; and N_0A (nuclei cm^{-2} s^{-1}), the three-dimensional nucleation constant. The values of these parameters for lead dioxide electrocrystallisation at 1480 mV *vs* SCE on a glassy carbon electrode are shown in Table 1. (only curves with the plateau well defined were employed). Other parameters shown in equation 1 are density, ρ (9.38 g cm^{-3}) and molar mass, M (239.2 g mol^{-1}) of lead dioxide.

As seen in Table 1, when the ultrasonic intensity increases, N_0A increases, the induction time decreases and the growth constant remains constant. These changes seem to be related with the generation of $OH^{\cdot}$ radicals during the water sonolysis [27]. The "hot spot" theory assumes that each cavitation bubble acts as a localised microreactor which, in aqueous systems, generates instantaneous temperatures of several thousand degree and pressures in excess of one thousand atmospheres. The "concentration" of cavitation bubbles produced by sonication using conventional laboratory equiptment is very small and so overall yields in this type of reaction are

low. Thus in the sonication of water small quantities of $OH^{\bullet}$ and $H^{\bullet}$ radicals are generated in the bubble and these undergo a range of reactions including the radicals adsorption onto the electrode surface. It has been reported by Velichenko et al [17] that a pausible mechanism for lead dioxide electrocrystallisation involving soluble intermediates could be:

$$H_2O \rightarrow OH_{ads} + H^+ + e^- \quad (2)$$

$$Pb^{2+} + OH_{ads} \rightarrow Pb(OH)^{2+} \quad (3)$$

$$Pb(OH)^{2+} + H_2O \rightarrow PbO_2 + 3H^+ + e \quad (4)$$

Taking into account that the concentration of $OH^{\cdot}$ radicals produced in sonicated solutions increases with the ultrasonic intensity [33], much more nucleation centers should be formed when the intensity of the ultrasound increases. However, these centres present the same growth constant for different values of ultrasonic intensity.

4. Conclusions

The results obtained show that the ultrasonic intensity strongly affects the lead dioxide electrodeposition kinetics on glassy carbon electrodes. This effect is different from the caused by the change of the electrode potential. More work is in progress in order to carry out a deeper study of the influence of power ultrasound on lead dioxide electrodeposition and on the electrochemical behaviour of C/PbO_2 obtained using different ultrasound frequencies and intensities.

5. Acknowledgements

The authors would like to thank “Ministerio de Ciencia y Tecnología” for financial support under project BQU2000-0460 and “Generalidad Valenciana” for financial support under project GR01-194.

References

1. P. Rüetschi, J. Electrochem. Soc. 139 (1992) 1347

2. A. M. Polcaro, S. Palmas, F. Renoldi, M. Mascia J. Appl. Electrochem. 29 (1999) 147

3. J. Iniesta, J. González-García, E. Expósito, V. Montiel, A. Aldaz Wat. Res. 35 (2001) 3291

4. S. Stucki, G. Theis, R. Kötz, H. Devantay, H. J. Christen, J. Electrochem. Soc. 132 (1985) 367.

5. N. Munichandraiah, S. Sathyanarayana J. Appl. Electrochem. 18 (1988) 314

6. F. Beck, in Electrochemistry of Lead, A. T. Kuhn Editor, Cap. 4, Academic Press, New York (1979)

7. G. H. Kelshall, ECRC/N 1060, Private Communication (1970)

8. M. Fleischmann, M. Liler, Trans. Faraday Soc. 54 (1958) 1370.

9. M. Fleischmann, H. R. Thirsk, Electrochim. Acta 1 (1959) 146.

10. M. Fleischmann, H. R. Thirsk, Electrochim. Acta 2 (1960) 22.

11. M. Fleischmann, J. R. Mansfield, H. R. Thirsk, H. G. E. Wilson, L. Wynne-Jones, Electrochim. Acta 12 (1967) 967.

12. H. A. Laitinen, N. H. Watkins, J. Electrochem. Soc. 123 (1976) 804.

13. S. A. Campbell, L. M. Peter, J. Electroanal. Chem. 306 (1991) 185.

14. H. Chang, D. C. Johnson, J. Electrochem. Soc. 136 (1989) 17.

15. H. Chang, D. C. Johnson, J. Electrochem. Soc. 136 (1989) 23.

16. A. B. Velichenko, D. V. Girenko, F. I. Danilov, Electrochim. Acta 40 (1995) 2803.

17. A. B. Velichenko, D. V. Girenko, F. I. Danilov, J. Electroanal. Chem. 405 (1996) 127.

18. A. B. Velichenko, S. V. Kovalyov, A. N. Gnatenko, R. Amadelli, D. V. Girenko, F. I. Danilov, Electrochim. Acta 454 (1998) 205.

19. H. Chang, D. C. Johnson, J. Electrochem. Soc. 136 (1989) 17.

20. J. González-García, F. Gallud, J. Iniesta, M. Montiel, A. Aldaz, A. Lasia Electroanalysis 13 (2001) 1258

21. J. Lee, H. Varela, S. Uhm, Y. Tak, Electrochem. Communications, 2 (2000) 646.

22. R. G. Compton, J. C. Eklund, F. Marken, Electroanalysis 9 (1997) 509.

23. J.S.Foord, R.Compton and F.Marken J.Electrochem.Soc 148 (2001) E66-E72.

24 C. R. S. Hagan, L. A. Coury Jr., Anal. Chem. 66 (1994) 399

25. H. Zhang, L. A. Coury, Jr. Anal. Chem. 65 (1993) 1552

26. T. J. Mason, Practical Sonochemistry, Ellis Horwood, Chichester, 1991.

27. J. González-García, J. Iniesta, A. Aldaz, V. Montiel, New J. Chem. 22 (1998) 343.

28. J. González-García, J. Iniesta, E. Expósito, V. García-García, V. Montiel, A. Aldaz, Thin Solid Films 352 (1999) 49.

29. J. González-García, V. Montiel, G. Sánchez-Cano, A. Aldaz, Spanish Pat. 9401259.

30. J. González-García, F. Gallud, J. Iniesta, V. Montiel, A. Aldaz, A. Lasia, New J. Chem. 25 (2001) 1195.

31. E. Agulló. Ph D. Universidad de Alicante, 2000.

32. Y. G. Li, W. Chrzanowski, A. Lasia, J. Appl. Electrochem., 26 (1996) 843.

33. H. Yanagida, Y. Masubuchi, K. Minagawa, T. Ogata, J.-I. Takimoto, K. Koyama Ultrasonics Sonochemistry 5 (1999) 133.

Captions

Power output /W cm^{-2}	t_0 /s	j_0 /mA cm^{-2}	N_0A /nuclei cm^{-2} s^{-1}	k /mol cm^{-2} s^{-1}
3.17	326±2	0.60±0.01	$(198.5\pm0.5)10^{3}$	$(3.532\pm0.003)10^{-8}$
4.81	311±2	0.65±0.02	$(690\pm3)10^{3}$	$(3.580\pm0.005)10^{-8}$

Table 1.- Kinetic parameters of electrocrystallization and growth of lead dioxide electrodeposition.

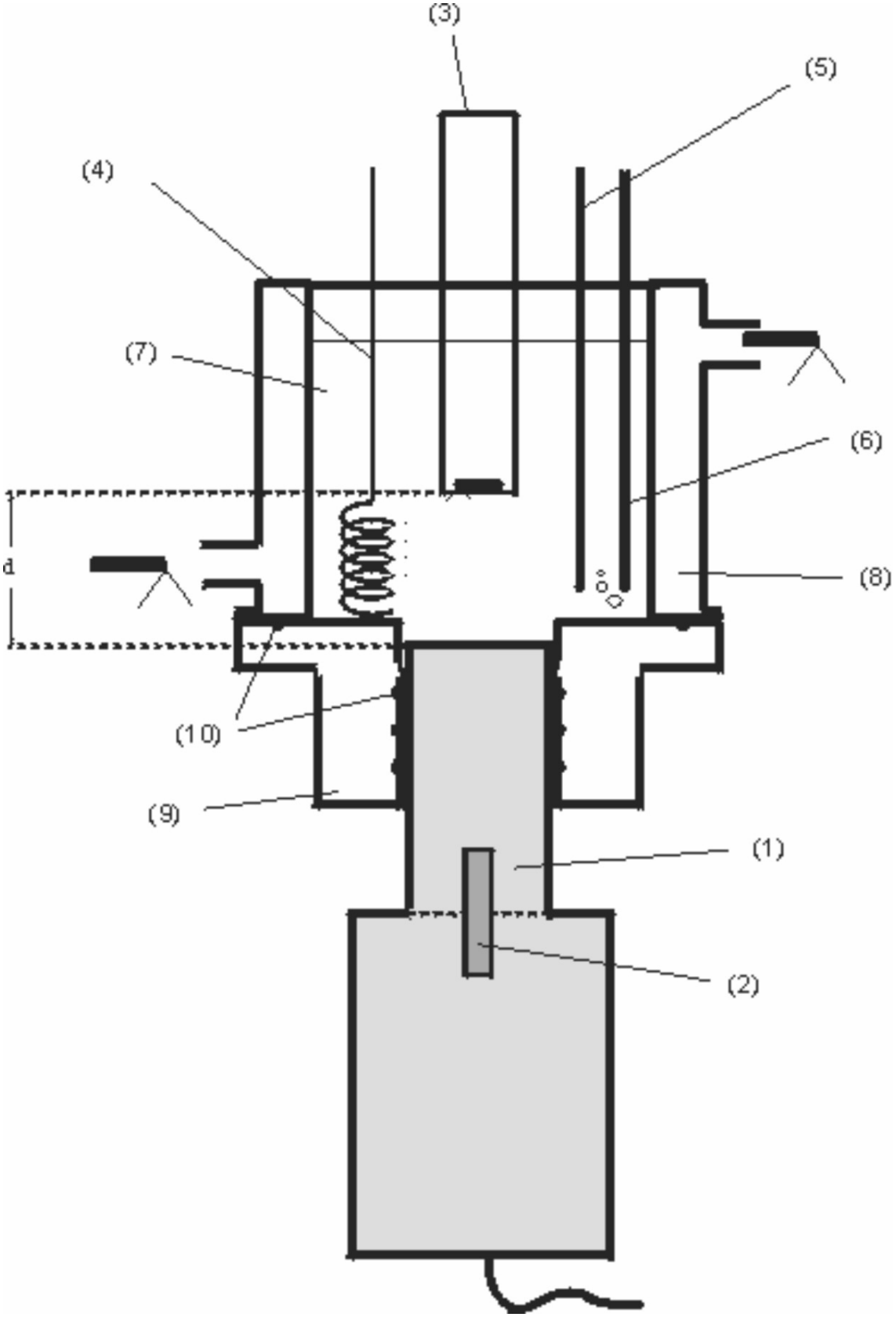
(3)
(5)
(4)
(7)
(6)
d
(8)
(10)
(9)
(1)
(2)

Figure 1.- Diagram of experimental set-up: (1) ultrasonic probe (2) transductor (3) working electrode (4) counter electrode (5) reference electrode/Luggin system (6) gas passing (7) electrolyte (8) cooling jacket (9) Teflon adapter (10) O-ring joints.

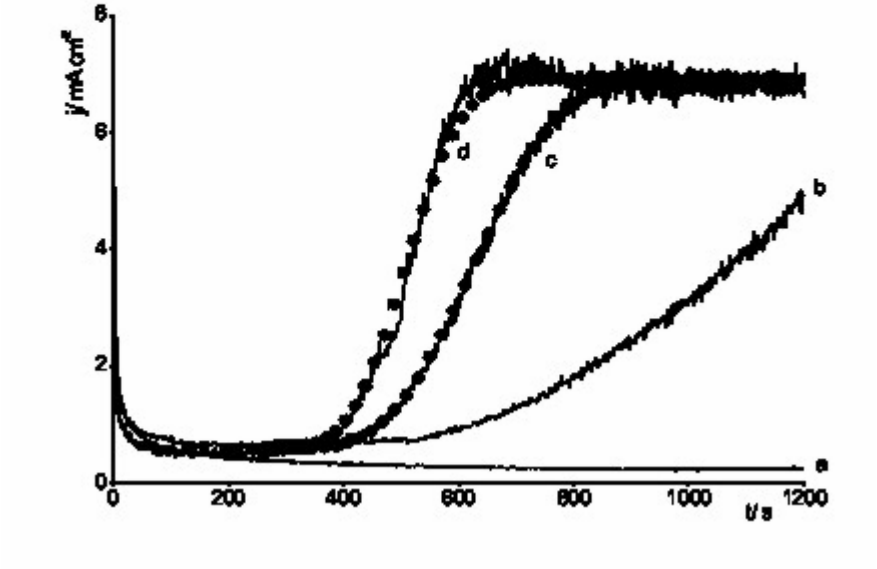

Figure 2.- Theoretical fit (•) of experimental curves (—) for lead dioxide electrodeposition (step final potential: 1480 mV *vs* SCE) in 0.1 mol dm^{-3} $Pb(NO_3)_2$ + 1 mol dm^{-3} HNO_3 at several ultrasonic intensities: (a) 0 W cm^{-2} (i. e. silent conditions); (b) 1.53 W cm^{-2} ; (c) 3.17 W cm^{-2} (d) 4.81 W cm^{-2}. Electrode diammeter 3 mm.

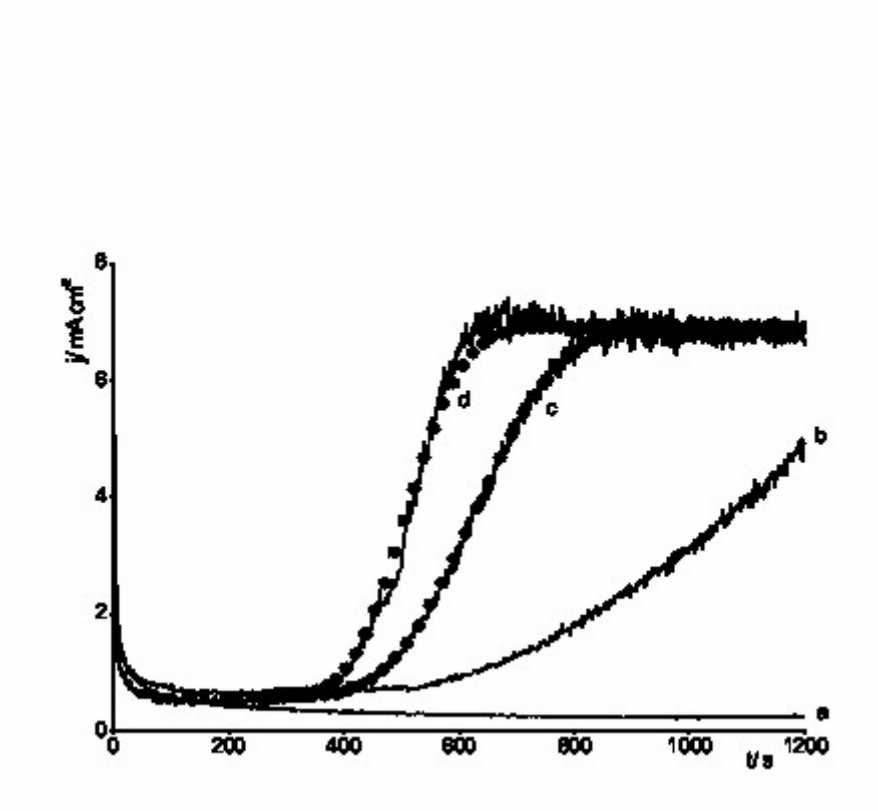

Figure 3.- Chronoamperometric curves for PbO_2 deposition in 0.1 mol dm^{-3} $Pb(NO_3)_2$ + 1 mol dm^{-3} HNO_3 at a glassy carbon electrode for different step final potentials (silent conditions): (a) 1480 mV *vs* SCE, (b) 1510 mV *vs* SCE, (c) 1520 mV *vs* SCE, (d) 1540 mV *vs* SCE. Electrode diammeter 3 mm.